

Adsorption from Oversaturated Aqueous Solution: Mean Force Molecular Simulations

Rupert Tscheliessnig, Lukas Geyrhofer, Martin Wendland, and Johann Fischer

Institut für Verfahrens-und Energietechnik, Universität für Bodenkultur, Muthgasse 107, A-1190 Wien, Austria

DOI 10.1002/aic.11557

Published online July 10, 2008 in Wiley InterScience (www.interscience.wiley.com).

The squeeze out of benzene from an aqueous solution to a planar graphite wall is considered by molecular simulations. The system contains 1–10 benzene molecules in water at $T = 300$ K and $p = 1$ bar corresponding to an oversaturation from 10 to 100. Local density profiles are obtained from the mean force method with a particle balance. For improving the accuracy, standard simulations results are incorporated into the mean force method. The resulting density profiles of benzene show a first peak at the wall with parallel and a second with perpendicular orientation of the molecules. For larger distances from the wall the structure levels out and for up to 40-fold oversaturation a limiting density of 25.8 ± 3.6 mmol/l is obtained. This value is in surprisingly good agreement with the experimental solubility limit of 22.8 mmol/l. The method may also be used for obtaining liquid–liquid equilibria. © 2008 American Institute of Chemical Engineers AICHE J, 54: 2479–2486, 2008

Keywords: adsorption/liquid, phase equilibrium, aqueous solutions, computer simulations (MC or MD), thermodynamics/statistical

Introduction

Adsorption from dilute solutions occurs in many engineering and biological applications. Examples are recovery of proteins via chromatography, adsorptive removal of organic impurities from water, or adsorption of pesticides from soil material. The challenge is to understand the structure of the adsorbate and to predict adsorption isotherms by molecular simulations. Of particular interest are systems with low solubility which occur frequently.

To calculate the structure of the adsorbate or the local density, one might think in first instant of using an unbiased histogram method which we call here as “standard molecular simulation.” With standard molecular simulations there may be problems in case of low solute concentrations for two rather different reasons with regard to the potential of mean

force (PMF) seen by the solute molecules. (a) In case there is no pronounced minimum in the PMF, the few solute particles stray around and hence give bad statistics as it happens, e.g., for spherical molecules.¹ (b) In case there is a strong barrier or a deep minimum in the PMF, the solute particles may not be able to cross the barrier or to leave the minimum which again gives an unreliable local density. To overcome these problems we have suggested the mean force (MF) method.^{1–4} In this method, one solute particle B is kept with one reference site at a fixed position and the MF exerted on this site from the other particles and from the wall is calculated. Next, the reference site is moved to a position closer to the wall and again the MF is calculated. Continuing, the reference site is moved on a path toward the wall and the MF values are recorded. Then, by integration of the MF along the path, the change of the PMF is obtained which is the change of the free energy along the path. Therefore the ratio of the local density of the solute at the end point to the local density at the starting point of the path can be calculated. Then, the absolute density values can be determined from a particle balance.⁴ This approach is in principle

Correspondence concerning this article should be addressed to J. Fischer at johann.fischer@boku.ac.at.

valid for any type of molecules, for any solute concentration and for any geometry. Regarding the geometry, our current interest is not so much in effects typical for narrow pores but rather in understanding the behavior at a single wall which confines the fluid. The slit pore geometry comes into play as a matter of convenience in the set-up of the simulations. To concentrate on the fluid at a single wall, however, the pore width has to be sufficiently large.

It has already been shown that the MF method allows the calculation of the adsorption isotherm for a dilute mixture in case of a 'simple system'. The latter means not too strong adsorption and molecules which do not demix in the bulk liquid. Actually we considered a model consisting of tetrahedral Lennard-Jones (LJ) solvent and linear LJ solute molecules in contact with a plane LJ 9/3 wall which mimics the adsorption of ethane from a dilute liquid solution in methane on graphite.⁴ The particle ratios of ethane to methane in the solutions considered there range from 1:399 to 40:360.

The item at issue is now more challenging, namely the adsorption of a solute from a mixture with very low solubility. As an example we consider the adsorption of benzene from an oversaturated aqueous solution to a planar graphite surface. With an oversaturated solution we mean a system in which the ratio of all solute particles to all solvent particles—adsorbed or in the bulk—exceeds the solubility limit. We remind that solubility⁵ of benzene in water at room temperature amounts to only 4.12×10^{-4} in mole fraction or 22.8 mmol/l which corresponds to one benzene molecule in 2428 water molecules. In case of oversaturation we expect that benzene molecules are both attracted by the adsorption force to the wall and squeezed out by their hydrophobicity from the water-rich bulk phase to the wall.

We want to mention that aqueous solutions of benzene have already been studied since some time by molecular simulations. The first papers known to us are from Linse et al.⁶ and Ravinshanker et al.⁷ and consider the structure of water molecules surrounding a benzene molecule by using parameterized intermolecular potentials from quantum mechanics. Other work⁸ on the structure of water molecules surrounding a benzene molecule was made with the AMBER force field.⁹ Investigations of the dynamics of benzene in water¹⁰ were made with the OPLS force field.¹¹ Linse¹² also studied the benzene-water interface and obtained complete demixing into two separate phases each of which has bulk fluid properties

Adsorption of benzene from an aqueous solution was first studied for the case of a NaCl solution and charged electrodes¹³ with emphasis on the effect of the electric field; in that work a version of the OPLS force field¹¹ was used. In a more recent paper,¹⁴ adsorption of benzene from water on Ni(111) and Au(111) surfaces was investigated. The interaction between the fluid molecules and the metal surfaces was taken from quantum mechanics, while for the interaction between the fluid molecules the GROMOS force field¹⁵ was used. In that paper,¹⁴ one benzene molecule and 2500 water molecules were treated by standard molecular simulations and relative local density profiles are given.

The adsorption of benzene from water on a graphite surface has already been considered in an earlier paper.³ In that work, only one benzene molecule was considered in the simulation box and only the relative local density could be cal-

culated. Here, however, we consider more benzene molecules in the simulation box and calculate the absolute local density.

Technically, a hybrid method is introduced for improving the accuracy of the results for more benzene molecules in the simulation box. In that case, standard simulations yield a density profile with small scattering close to the wall but do not show any benzene molecules in the bulk which does not allow a determination of the bulk fluid density. On the other hand, MF calculations as described earlier could be performed in the whole box with, however, less accuracy than the standard simulations close to the wall. These results suggest coupling both methods on the level of the MF.

In the next section the theory will be presented. Thereafter, the molecular model of the liquid mixture at the graphite wall and the simulation methodology will be specified. Finally, results will be given.

Theory

As already mentioned in the Introduction, in case of more benzene molecules in the simulation box a hybrid method will be introduced in order to improve the accuracy of the results. The idea of this hybrid method is to couple the results of standard simulations for the local density close to the wall with MF results for more remote distances. In this section we first give a summary of the MF method as it was used previously for the determination of the absolute values of the local densities and for the calculation of an adsorption isotherm.⁴ Thereafter, we explain how the MF can also be calculated from a known local density profile.

We consider a fluid mixture with solvent A-particles and solute B-particles in contact with a wall. In the MF-method, one solute particle B is kept with one reference site at a fixed position \mathbf{r} and the MF $\langle \mathbf{F}_B(\mathbf{r}) \rangle$ exerted on this site from the other particles and from the wall is calculated. For clarity in the nomenclature we denote these simulations and the resulting MF values as constrained. Next, the reference site is moved to a position closer to the wall and again the MF is calculated. Continuing, the reference site is moved on a path and the MF values are recorded. In principle, this path is arbitrary but should reasonably be chosen according to the geometry of the model. Then, by integration over the MF along this path denoted by s , the change of the PMF Δw is obtained as

$$\Delta w = - \int \langle \mathbf{F}_B(s) \rangle \bullet ds, \quad (1)$$

wherein the change Δ refers to the difference between the end point \mathbf{r}_b and the starting point \mathbf{r}_a of the path s . Next, it is known that the local density $n_B(\mathbf{r})$ is related to the change of the PMF according to

$$\Delta w = -kT \Delta \ln n_B(\mathbf{r}), \quad (2)$$

or

$$n_B(\mathbf{r}_b) = n_B(\mathbf{r}_a) \exp\{-\beta \Delta w\}, \quad (3)$$

with Δw given by Eq. 1, $\beta = 1/kT$, and a still unknown value of $n_B(\mathbf{r}_a)$. To determine the absolute value of the local den-

Table 1. Potential Parameters for Benzene, Water, and Carbon According to CHARMM21¹⁷

Molecule	Bond	Bond Length, L (nm)	Site	Site-Site Energy $\epsilon_{\alpha\beta}/k$ (K)	Site-Site Diameter $\sigma_{\alpha\alpha}$ (nm)	Charge q (e)
C ₆ H ₆	C—C	0.13870				
C ₆ H ₆	C—H	0.10800				
C ₆ H ₆			C	25.1778	0.363487	−0.10
C ₆ H ₆			H	21.1494	0.236979	+0.10
H ₂ O	O—H	0.096				
H ₂ O			O	76.5	0.313596	−0.834
H ₂ O			H	—	—	+0.417
C (graphite)			C	25.1778	0.363487	

Benzene is modeled as ring with six C- and six H-atoms, each of which is a Lennard-Jones interaction site and carries a partial charge. Water is described by the TIP3P model, which assumes a LJ interaction site on the oxygen atom and partial charges on the hydrogen and the oxygen atoms with an angle $\vartheta = 104.5^\circ$ between the O—H bonds. The wall consists of carbon atoms which are also modeled as LJ particles. Given are the Lennard-Jones 12/6 parameters $\epsilon_{\alpha\alpha}$ and $\sigma_{\alpha\alpha}$ between like interaction sites α , bond lengths L , and partial electric charges q .

sity $n_B(\mathbf{r})$ we use the particle balance which says that the volume integral over the local density $n_B(\mathbf{r})$ has to be the total number of B-particles in the given volume V

$$\int n_B(\mathbf{r}) d\mathbf{r} = N_B. \quad (4)$$

By insertion of Eq. 3 into Eq. 4 one obtains

$$n_B(\mathbf{r}_a) \int \exp\{-\beta\Delta w\} d\mathbf{r} = N_B, \quad (5)$$

from which the absolute value of the local density $n_B(\mathbf{r}_a)$ can be determined and therefrom via Eq. 3 the absolute value of the local density at any point \mathbf{r} in the fluid. When the starting point \mathbf{r}_a is in the bulk fluid, the absolute value of the local density $n_B(\mathbf{r}_a)$ is just the bulk fluid density n_{Bb} of component B.

In case that the constrained simulations of the MF do not give sufficiently accurate results, the MF may also be calculated by differentiation of the density profile obtained from standard, i.e., from unconstrained simulations. Forming the logarithm of Eq. 3 yields

$$\ln n_B(\mathbf{r}_b) = \ln n_B(\mathbf{r}_a) - \beta\Delta w, \quad (6)$$

After insertion of Eq. 1 into Eq. 6 one obtains

$$\ln n_B(\mathbf{r}_b) = \ln n_B(\mathbf{r}_a) + \int \langle \mathbf{F}_B(s) \rangle \bullet d\mathbf{s}, \quad (7)$$

and by differentiation of Eq. 7 one obtains the MF as

$$\langle \mathbf{F}_B(\mathbf{r}) \rangle = (1/\beta) \nabla_{\mathbf{r}} \ln n_B(\mathbf{r}), \quad (8)$$

where $\nabla_{\mathbf{r}}$ denotes the gradient of $n_B(\mathbf{r})$. For clarity in the nomenclature, we call this method inverse mean force (IMF) method and the resulting MF values IMF values. Note, that Eq. 8 corresponds just to the Born-Green-Yvon equation which was successfully used for a theoretical description of various interfacial phenomena.¹⁶

Finally, the adsorption excess Γ per unit area on a surface A can be defined as

$$\Gamma = (1/A) \int [n_B(\mathbf{r}) - n_{Bb}] d\mathbf{r}. \quad (9)$$

Model and Simulation Methodology

The systems investigated consist of N_B benzene molecules and N_A water molecules in a graphite slit pore of width L . The coordinate perpendicular to the walls is z which runs from zero at the left to L at the right wall. Benzene is modeled as ring with six C- and six H-atoms, which are taken as LJ interaction sites with additional partial charges. Water is described by the TIP3P model, which assumes a LJ interaction site only on the oxygen atom and partial charges on the hydrogen and on the oxygen atoms. The wall consists of carbon atoms which are also modeled as LJ particles. All parameters are taken from CHARMM21¹⁷ and given in Table 1. All interactions between unlike sites are assumed as LJ-interactions with parameters $\epsilon_{\alpha\beta}$ and $\sigma_{\alpha\beta}$ according to the Lorentz-Berthelot combining rules^{18,19} and as electrostatic interactions between the partial charges. While other authors dealing with benzene in water used e.g. parameterized quantum mechanical potentials,^{6,7} or empirical force fields like GROMOS,¹⁵ AMBER,⁹ or OPLS¹¹ we decided to use again³ the CHARMM force field as a recent study by Martin²⁰ came to the conclusion “The CHARMM and TraPPE force fields are recommended to people interested in performing fluid phase simulations.” All interactions between the fluid molecules, the LJ as well as the electrostatic interactions, were cut off at a distance of 1.2 nm which in all cases considered here is slightly smaller than $L/2$ with L given in Table 2.

Moreover, to simplify the interaction between a fluid particle and a graphite wall Steele has suggested²¹ to replace the discrete set of graphite carbon atoms by a continuous distribution of atoms in an infinite half-space with atom density $\rho_c = 110.3 \text{ nm}^{-3}$. The wall potential for a site s in the fluid (C and H for benzene, O for water) is obtained by averaging over the unlike LJ interactions between this site and all carbon atoms in the half-spaces $z \leq 0$ and $z \geq L$. The unlike interaction parameters ϵ_{cs} and σ_{cs} are again obtained via the Lorentz-Berthelot combining rules.^{18,19} The resulting wall potential u_w between the plane graphite wall bounded by $z = 0$ and an interaction site s at a distance $z \geq 0$ from the wall is then obtained as

$$u_w = (2/3) \pi \epsilon_{cs} \rho_c \sigma_{cs}^3 [(2/15)(\sigma_{cs}/z)^9 - (\sigma_{cs}/z)^3]. \quad (10)$$

An analogous expression holds for the potential from the wall bounded by $z = L$. The present CHARMM21¹⁷ param-

Table 2. Number of Benzene Particles N_B and Widths of the Simulation Boxes L as well as Results for the Integral K^* , the Benzene Density $n_B(z_a)$ and the Surface Excess Γ

N_B	L (nm)	K (nm)	$n_B(z_a)$ (mmol/l)	Γ ($\mu\text{mol}/\text{m}^2$)
1	2.472	10.25	26.5	0.25
2	2.478	17.25	31.4	0.51
3	2.484	35.65	22.6	0.79
4	2.492	47.27	22.6	1.05
6	2.506	81.42	19.5	1.57
8	2.520	52.52	39.8	2.05
10	2.533	48.90	52.9	2.54

* K is calculated from Eq. 13 taking $z_b = 0.25$ and $z_a = 1.2$ nm.

ters for ε_{cc} and σ_{cc} are given in Table 1 and are very close to the original values given by Steele.²¹ As an alternative to the 9/3 potential of Eq. 10 we could have also used the $\Sigma 10/4$ potential²¹ which is obtained from a continuous distribution of the carbon atoms in the basal planes and from summing up the contributions from successive planes. The well of the 9/3 potential is somewhat broader but less deep than the well of the $\Sigma 10/4$ potential.

Molecular dynamics (MD) simulations were performed with the code MACSIMUS²² into which the MF-method had been implemented. A cubic simulation box of side length L with $N_B = 1, 2, 3, 4, 6, 8$, and 10 benzene molecules and $N_A = 500$ water molecules was considered. The temperature was kept constant at 300 K using the Berendsen friction thermostat.²³ The side length L was chosen such that the pressure was about 1 bar which means that with increasing number of benzene particles N_B the side length L increased from 2.47 to 2.53 nm. Periodic boundary conditions were used in the directions parallel to the LJ walls, and the length of the integration time steps was ~ 1.67 fs. The calculated density profiles refer for benzene to its center of mass and for water to the oxygen atom.

At this point it may be helpful to get some physical understanding of the situation. First, we consider the surface area of a benzene molecule. If this surface area is calculated approximately as $A_{C_6H_6} = r^2\pi$ with $r = L_{CC} + L_{CH} + 0.5\sigma_{HH}$ and L_{CC} , L_{CH} , and σ_{HH} are taken from Table 1, a value of $A_{C_6H_6} = 0.419 \text{ nm}^2$ is obtained which is in good agreement with the classical value of 0.408 nm^2 and a recent estimate of 0.423 nm^2 .²⁴ If we take an average cube length L of 2.50 nm, the base area A of the cube is 6.25 nm^2 which means that about 15 benzene molecules with parallel orientation to the wall can be placed in one layer. Moreover, a closer examination of simulations for several benzene molecules in aqueous solution in the slit between the graphite walls showed that the benzene molecules either moved rather quickly to the walls or formed a cluster in the water which after a certain time also moved to one of the walls.

For the constrained MF simulations, $N_A = 500$ water molecules and $(N_B - 1)$ benzene molecules which could move freely were placed inside the simulation box. One additional benzene molecule was considered as reference molecule and its center of mass was kept at fixed positions with distance z from the wall while it was allowed to rotate freely. The $(N_B - 1)$ unconstrained benzene molecules were initially inserted next to the left graphite wall and remained in that area during the simulation runs. On the other side of the

pore, no benzene molecules were placed and none moved there during the simulation runs. This asymmetric preparation of the system is justified by the observation that for only a few benzene molecules at the wall we could not observe any influence of the benzenes at the wall on the reference benzene molecule in the center of the pore. An explanation for this observation could be that the interaction between the few benzenes at the wall and the reference benzene in the center of the pore is screened by the intermediate water. The calculation of the MF on the reference benzene molecule was started at the distance $z_a = 1.2$ nm which is close to the center of the pore. The reference molecule was then moved stepwise closer to the wall down to a distance $z_b = 0.25$ nm on a path perpendicular to the wall. The resulting MF values which for planar geometry only have a z -component $\langle F_B(z) \rangle$ are integrated according to Eq. 1 to yield the PMF

$$\Delta w = w(z) - w(z_a) = - \int_{z_a}^z \langle F_B(s) \rangle ds. \quad (11)$$

Then, following Eq. 5, the absolute value of the local density $n_B(z_a)$ at z_a is obtained from

$$n_B(z_a) A K = N_B, \quad (12)$$

with $A = L^2$ and K being given by integration over the Boltzmann-factor of the PMF

$$K = \int_{z_b}^{z_a} \exp\{-\beta\Delta w\} dz. \quad (13)$$

The local density $n_B(z)$ at any point z is then given as

$$n_B(z) = n_B(z_a) \exp\{-\beta\Delta w\}. \quad (14)$$

In case that the starting position z_a is in the bulk fluid, the absolute value of the local density $n_B(z_a)$ is just the bulk fluid density n_{Bb} of component B. Regarding the limit $z_a = 1.2$ nm, which is close to the center of the pore, no influence of the walls could be seen for small numbers of N_B , at least up to $N_B = 4$. On the other hand, for $z_b = 0.25$ the PMF is already that high that $\exp\{-\beta\Delta w\}$ is nearly zero there.

The main computational task was the calculation of the MF on the reference benzene molecule for a series of 200 grid points at equidistant positions z_i , $i = 1, 2, \dots, 200$ in the interval between the pore center $z = L/2$ and $z_b = 0.25$ nm, which required appropriate preparation of the initial state of the system for each grid point. In principle, a run was made with the reference molecule at z_i . After the run the reference molecule was drawn at fixed x and y by an external force from position z_i to z_{i+1} . Because of this move of the reference molecule, the system was in slight nonequilibrium and hence an equilibration run of 16 ps corresponding to 9600 time steps was performed. Thereafter the production run followed for z_{i+1} lasted between 50 and 110 ps corresponding to 30,000 up to 66,000 time steps. For $N_B = 1$ and 2, the method was applied in this form. In addition to moving the reference molecule from the center of the pore to the wall on 200 grid points z_i , it was also moved back again on

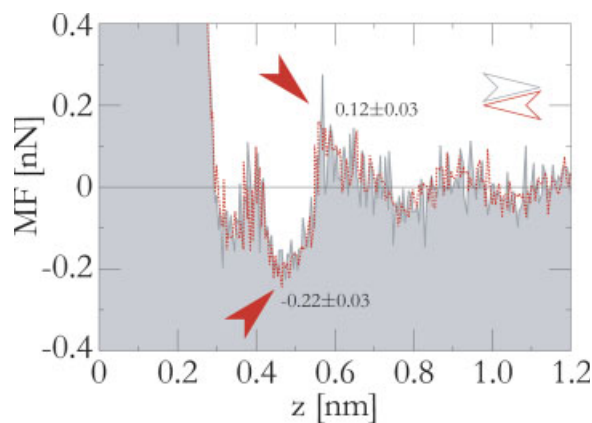


Figure 1. MF values from constrained simulations as function of the wall-particle distance z for one benzene molecule in 500 water molecules.

The reference particle was moved toward the wall (—) and withdrawn from the wall (— with gray body). [Color figure can be viewed in the online issue, which is available at www.interscience.wiley.com.]

200 grid points to have a consistency check. For $N_B \geq 2$, i.e. for $N_B = 2$ too, we used a modified method to speed up the computations by parallel runs. Hence, we divided the whole interval from $z = L/2$ to $z_b = 0.25$ into 10 equidistant subintervals in order to perform the simulations in the subintervals parallel. In this case the reference molecule was drawn directly from $L/2$ to the first grid point of the subinterval which was thought to lead to a stronger nonequilibrium of the initial state. Hence, for these grid points the velocities of all freely moving molecules were first adjusted to a Maxwell-Boltzmann distribution. Moreover, the production runs were extended up to 150 ps which corresponds to 90,000 time steps. For the subsequent grid points the procedure was the same as described for the case without subintervals.

As already shown by Eq. 8, the MF may also be calculated by differentiation of the density profile obtained from unconstrained simulations. These density profiles show rather small scattering close to the wall. After the first layer of parallel and perpendicular oriented benzenes at the wall, however, no benzene molecules could be found any more in the unconstrained simulations which prohibited the determination of the bulk density. On the other hand, direct MF calculations by constrained simulations could be performed in the whole box with, however, less accuracy than the standard simulations close to the wall. As a consequence, we coupled both methods on the MF level. Technical details of the coupling will be given in the next section in connection with the presentation of results.

Results and Discussion

First, we consider the results for one benzene molecule in 500 water molecules from constrained simulations. We remind that this case has already been studied,³ but at that time we could not yet give absolute density values. There, the main findings on the structure of benzene were that in the first peak of $n_B(z)$ close to the wall the molecules are

mainly oriented parallel and in the second perpendicular to the wall. Benzene molecules more remote from the wall were in almost perpendicular orientation bridging two water layers. The water structure was also given previously.³ The essential progress of the present work is that we now obtain absolute values for the local density profile $n_B(z)$, while previously we could only give relative values for the local density.

Let us now consider the present results for one benzene molecule in 500 water molecules in detail. The MF values in nanonewton (nN) from the constrained simulations are shown in Figure 1 as function of the distance from the wall in nm. Positive MF values are repulsive with respect to the wall, negative are attractive. The reference molecule was moved from the center of the pore to the wall on 200 grid points z_i and back again on 200 grid points to have a consistency check. The figure contains the MF results of both paths, which have already been averaged over distances of 0.01 nm, i.e. in essence averages of two MF results at distances z_i and z_{i+1} are shown. It is seen that the results show some scattering but also a clear structure. Besides the strong repulsive MF close to the wall, a minimum in the MF of -0.22 ± 0.03 nN occurs at $z = 0.47$ nm and a relative maximum of 0.12 ± 0.03 nN at $z = 0.57$ nm, where the uncertainty refers to the scattering of several subsequent grid points. These results basically agree with those shown in Figure 1 of the previous paper.³ From the MF, the PMF is obtained by integration according to Eq. 11 which smoothes the results. The present PMF is rather similar to that which was already shown and discussed previously.³ Subsequently the Boltzmann factor of the PMF is integrated according to Eq. 13 and with the particle balance from Eq. 14 the absolute local density profile of benzene $n_B(z)$ is obtained. These results are shown in Figure 2 which has two different scales on the y-axis: for larger distances from the wall the scale is enlarged by a factor of 62.5. Again, high similarity exists between the previous relative³ and the present absolute density profile. Clearly, the new result is the absolute value of the local density of benzene which is expressed in Figure 2 in mol/l (lhs) or mmol/l (rhs). We also see from Figure 2 that at $z_a = 1.2$ nm the local benzene density has nearly

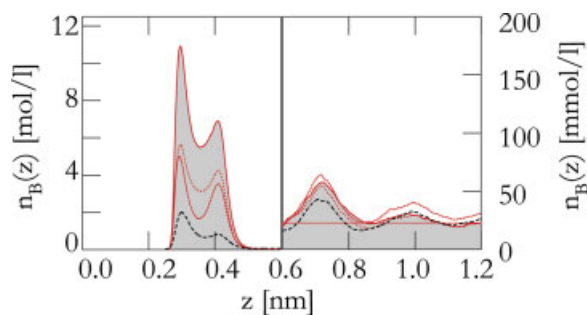


Figure 2. Density profiles of benzene $n_B(z)$ for 1–4 benzene molecules in solution, — $N_B = 1$, • • • $N_B = 2$, — • — $N_B = 3$, — $N_B = 4$.

The rhs scale is 62.5 times larger than the lhs scale. The horizontal line is the experimental solubility limit. [Color figure can be viewed in the online issue, which is available at www.interscience.wiley.com.]

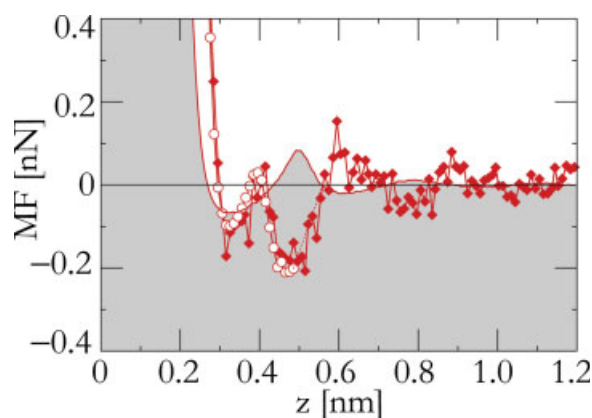


Figure 3. MF values as function of the wall-particle distance z for three benzene molecules in 500 water molecules.

◆ Constrained MF for benzene, ○ unconstrained IMF for benzene, — (with gray body) unconstrained IMF for water, — — — interpolated MF. [Color figure can be viewed in the online issue, which is available at www.interscience.wiley.com.]

smoothed out and arrived at a value $n_B(z_a) = 26.5$ mmol/l. The numbers for the box length L , for the integral K defined in Eq. 13, as well as for the absolute density $n_B(z_a)$ and the surface excess Γ are given in Table 2. The exciting finding is that the calculated value $n_B(z_a) = 26.5$ mmol/l is rather close to the experimental solubility limit of $n_B(z_a) = 22.8$ mmol/l.

So far we have obtained the following picture. As the benzene molecule is restricted to the left half of the pore, we have a benzene to water ratio of about 1:250 or 10-fold oversaturation. The simulations have shown that the benzene is squeezed out or attracted to the wall such that its density in some distance from the wall just corresponds to the solubility limit. To validate this picture we now increase the oversaturation by inserting more benzene molecules into the water.

We now proceed to the evaluation for two and more benzene molecules in solution, where the MF from constrained and the IMF values from unconstrained simulations were coupled. For more than two benzene molecules always the same coupling procedure was used which is a little more complicated than for two benzene molecules. Hence we start by explaining the coupling for $N_B = 3$ and describe the simplification for $N_B = 2$ later. For $N_B = 3$ we first calculated the MF values directly from constrained simulations. For the preparation of the initial state, we used the modified method in which the whole interval from $z = L/2$ to $z_b = 0.25$ was subdivided into 10 equidistant subintervals. Two, i.e. $(N_B - 1)$, freely moving benzene molecules were inserted into the water close to the left wall and the reference molecule was fixed at positions z_i . The resulting MF values are presented in Figure 3 where for clarity MF averages of two subsequent grid points are shown. We recover a similar profile for the MF as for $N_B = 1$ shown in Figure 1. After the MF calculations with constrained simulations, we calculated the local density profiles of benzene and water with unconstrained simulations and determined therefrom the IMF values via Eq. 8, which are shown for benzene and water in Figure 3,

too. We observe that the IMF-values for benzene are restricted to distances close to the wall as in the unconstrained simulations no benzenes could be found further away; the largest distance for which a reliable IMF value is available is called z_{limf} . On the other hand, for water the IMF values are available throughout the pore. The coupling between the constrained MF and the unconstrained IMF values is determined by the previous observation³ that for distances beyond the first benzene layer, the maxima in the local density $n_B(z)$ of benzene are just in the minima of the local density of water and vice versa which is confirmed by the present results. In particular we observe a water maximum and a benzene minimum at a distance z_m close to 0.55 nm, which means that the MF values of benzene and water have to be zero just at z_m . The recipe for coupling the constrained MF with the unconstrained IMF values is the following. We take the IMF values for $z \leq z_{limf}$ and the constrained MF values for $z > z_m$. In the interval $z_{limf} < z < z_m$ in principle the constrained MF values could be taken which, however, are strongly scattering there. Hence it seemed appropriate to make a linear interpolation for the MF in this interval which is also indicated in Figure 3 as the dashed line. In case of $N_B = 2$, the constrained MF values obtained from both methods to move the reference molecule (cf. previous section) ran smoothly into the IMF values and hence the interpolation between z_{limf} and z_m was not required.

Thus, after determining the MF values for all distances $z \leq 1.2$ nm, the further evaluation was done as described earlier for $N_B = 1$. The PMF was obtained by integration and therefrom the relative local density. Finally, the absolute value $n_B(z)$ was calculated by using the particle balance. The numbers for the box lengths L , for the integrals K , as well as for the absolute densities $n_B(z_a)$, and the surface excess values Γ are given in Table 2. The density profiles for $N_B = 2, 3$, and 4 are shown in Figure 2 together with the density profile for $N_B = 1$. We remind that the rhs scale is enlarged by a factor of 62.5. The density profiles for $N_B = 4$ is repeated in Figure 4 which also shows the profiles for $N_B = 6, 8$, and 10. In Figure 4 the rhs scale is the same as in Figure 2 and 150 times larger than the lhs scale.

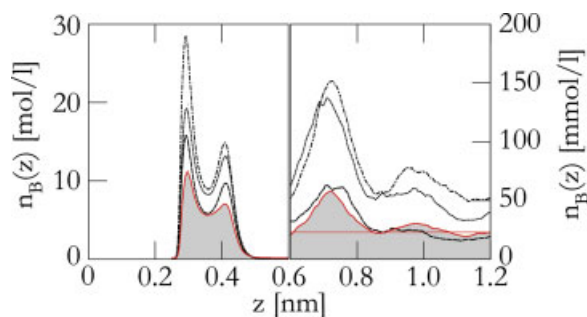


Figure 4. Density profiles of benzene $n_B(z)$ for 4, 6, 8, and 10 benzene molecules in solution, — $N_B = 4$, — — — $N_B = 6$, • • • $N_B = 8$, — • — $N_B = 10$.

The rhs scale is 150 times larger than the lhs scale. The horizontal line is the experimental solubility limit. [Color figure can be viewed in the online issue, which is available at www.interscience.wiley.com.]

The above results for one benzene molecule ($N_B = 1$) showed clearly that in case of oversaturation the benzene molecules are squeezed out until the benzene density in some distance from the wall just corresponds to the solubility limit. This picture is confirmed by Figure 2 for $N_B = 2, 3$, and 4. From the left hand side we see that close to the wall the density profiles $n_B(z)$ scale approximately linear with N_B , while the rhs shows that in some distance away from the wall the oscillations in $n_B(z)$ have smoothed out and all profiles approach a value which is close to the experimental solubility limit. Taking the $n_B(z_a)$ values at $z_a = 1.2$ nm for $N_B = 1, 2, 3$, and 4 from Table 2 and averaging them we obtain $\langle n_B(z_a) \rangle_{1-4} = 25.8 \pm 3.6$ mmol/l which agrees surprisingly well with the experimental value for the solubility limit of 22.8 mmol/l. Consistent with these findings, the surface excess Γ given in Table 2 increases approximately linearly with N_B which simply shows that nearly all benzene is sitting at the wall.

We mentioned earlier that the density profiles $n_B(z)$ scale approximately linear with N_B but this statement is not quite justified for $N_B = 2$ and also the $n_B(z_a)$ value has its strongest deviation from $\langle n_B(z_a) \rangle_{1-4}$ for $N_B = 2$. We believe that this is a statistical uncertainty with perhaps some physical reason. In case of $N_B = 1$, there are no freely moving benzene molecules in the solution and the reference molecule sees besides the wall only water molecules which should yield good statistics for the MF on the reference benzene. In case of $N_B = \geq 3$, there are two or more freely moving benzene molecules which form a cluster at the wall. In case that the reference molecule approaches the wall, the freely moving molecules adjust their positions such that the reference molecule becomes more and more the center of the cluster with decreasing distance from the wall. Again, this should yield a reasonable statistics for the MF on the reference benzene. On the other hand, if $N_B = 2$, the force on the reference benzene comes besides from the wall and the water molecules from only one free benzene which may be the reason for worse statistics in the MF.

In Figure 4, the density profiles $n_B(z)$ are shown for $N_B = 4, 6, 8$, and 10, which corresponds to 40- to 100-fold oversaturation of the solution. Again we see on the lhs an approximately linear increase in the local density $n_B(z)$ with N_B close to the wall. On the rhs the density $n_B(z)$ approaches again the experimental solubility limit at $z_a = 1.2$ nm for $N_B = 4$ and 6. For $N_B = 8$ and 10, however, the density profile shows still some oscillations in approaching the center of the pore and remains at higher values than for less solute benzene molecules in approaching the center of the pore. We believe that this is consequence of the width of the pore and somehow reflects the transition from the behavior at a single wall to the behavior in a pore. The latter, however, can not be assessed properly by our one-sided loading of the pore with benzene molecules. We expect that for a wider pore the density profile would even for more benzene particles again relax to the experimental solubility limit.

Finally, we show in Figure 5 the values $n_B(z_a)$ at $z_a = 1.2$ nm for 1–10 benzene molecules in comparison with the experimental solubility limit. This supports the finding that up to six benzenes, i.e., up to 60-fold oversaturation, the benzenes are squeezed out to the wall and that at the distance

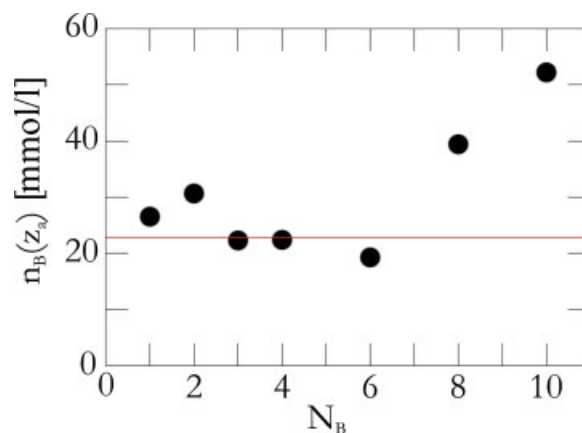


Figure 5. Local densities of benzene $n_B(z_a)$ at $z_a = 1.2$ nm for 1–10 benzene molecules in aqueous solution.

The horizontal line is the experimental solubility limit. [Color figure can be viewed in the online issue, which is available at www.interscience.wiley.com.]

$z_a = 1.2$ nm from the wall the density within some simulation uncertainty is close to the experimental solubility limit.

The question remains on the influence of the wall potential on the results. The most interesting result found is that the local density of benzene in the center of the pore agrees very well with the experimental solubility. As the solubility is a bulk fluid property this result will not be changed by the choice of the wall potential. Regarding the structure close to the wall we believe that the peaks in the local density would be somewhat higher and more narrow in case of the $\Sigma 10/4$ potential²¹ in comparison with the 9/3 potential²¹ due to the shape of the potential wells mentioned earlier. The thermodynamic effect e.g. on the adsorption isotherm for lower overall benzene concentration remains still to be explored but is believed to be small.

Summary and Conclusions

In a previous article⁴ and in this article we calculated the absolute local density $n_B(z)$ of a solute B in a dilute solution close to an adsorbing surface by using the MF method together with the particle balance. In the previous article,⁴ we considered ethane dissolved in methane which is a completely miscible solution and demonstrated how and with which accuracy the adsorption isotherm can be calculated. In the present article we considered benzene in water which has only a low solubility and found that nearly all the benzene is adsorbed at the wall and that in some distance away from the wall the density of the benzene agrees surprisingly well with the experimental solubility limit.

The formal problem is the calculation of the PMF seen by one molecule in a solution close to a wall. There is a similarity between this problem and the calculation of the PMF between two molecules in solution which was recently reviewed for the case of two methane molecules in water.²⁵ It should be mentioned that it was also found there²⁵ that the calculation of the PMF via constrained simulations for the MF is the most accurate method. The differences between

that system and ours are as follows: (a) our adsorption problem can be treated immediately in Cartesian coordinates which avoids a lot of problems, (b) we can easily introduce more solute molecules. Moreover, as far as the application of the MF method to adsorption is concerned, we are not aware of any other work.

The calculation of the MF by simulations requires some care in particular with respect to the preparation of the initial state for each run which should be in equilibrium. It might be that the simulation time could be shortened by using the Jarzynski equation²⁶ which allows the calculation of the equilibrium PMF from nonequilibrium simulations.

The newly developed method allows the rather accurate calculation of adsorption isotherms in particular from dilute solutions for systems ranging from complete miscibility to such with rather low solubility. Moreover, the method can also be used for obtaining liquid–liquid equilibria in case of low solubilities.

Topics for further research are the investigation of the effect of the wall adsorption strength on the solute. In case of adsorption of benzene from water, e.g., a stronger adsorbing wall than the present could attract even more solutes from the solution and as a consequence the bulk fluid density could remain beyond the solubility limit. Finally, it might also be challenging to use MF simulations for developing engineering models for adsorption from solutions to improve previous models based either on molecular interactions²⁷ or on mixture thermodynamics.²⁸

Acknowledgments

The authors thank Prof. J. Kolafa, Prague, for making MACSIMUS available to them and for his continuous help therewith. Financial support by Deutsche Forschungsgemeinschaft for the project “Adsorption aus wässrigen Lösungen,” Az Fi 287/13-2, within the priority research programme “Molekulare Modellierung und Simulation in der Verfahrenstechnik” as well as the allocation of computer time at JUMP, project ID hvi020, by the John von Neumann Institute für Computing, Jülich, Germany, are gratefully acknowledged.

Literature Cited

1. Billes W, Bazant-Hegemark F, Mecke M, Wendland M, Fischer J. Change of free energy during adsorption of a molecule. *Langmuir*. 2003;19:10862–10868.
2. Billes W, Tscheliessnig R, Fischer J. Molecular simulation of adsorption from dilute solutions. *Acta Biochim Pol*. 2005;52:685–689.
3. Tscheliessnig R, Billes W, Wendland M, Fischer J, Kolafa J. Adsorption of benzene from an aqueous solution. *Mol Simul*. 2005;31:661–666.
4. Billes W, Tscheliessnig R, Sobczak L, Wendland M, Fischer J, Kolafa J. Adsorption isotherms for dilute solutions via the Mean Force method. *Mol Simul*. 2007;33:655–666.
5. Maczynski A, Shaw DG, Goral M, Wisniewska-Gocłowska B, Skrzecz A, Owczarek I, Blazej K, Haulait-Pirson MC, Heftner GT, Maczynska Z, Szafranski A, Tsionopoulos C, Young CL. IUPAC-NIST Solubility Data Series 81. Hydrocarbons with water and seawater—revised and updated, Part 2: Benzene with water and heavy water. *J Phys Chem Ref Data*. 2005;34:477–552.
6. Linse P, Karlström G, Jönsson B. Monte Carlo studies of a dilute aqueous solution of benzene. *J Am Chem Soc*. 1984;106:4096–4102.
7. Ravinshanker G, Mehrotra PK, Mezei M, Beveridge DL. Aqueous hydration of benzene. *J Am Chem Soc*. 1984;106:4102–4108.
8. Meng EC, Kollmann PA. Molecular dynamics studies of the properties of water around simple organic molecules. *J Phys Chem*. 1996;100:11460–11470.
9. Cornell WD, Cieplak P, Bayly CI, Gould IR, Merz KM Jr, Ferguson DM, Spellmeyer DC, Fox T, Caldwell JW, Kollmann PA. A second generation force field for the simulation of proteins, nucleic acids and organic molecules. *J Am Chem Soc*. 1995;117:5179–5197.
10. Laaksonen A, Stilbs P, Wasylishen RE. Molecular motion and solvation of benzene in water, carbon tetrachloride, carbon disulfide and benzene: a combined molecular dynamics simulation and nuclear magnetic resonance study. *J Chem Phys*. 1998;108:455–468.
11. Jorgensen WL, Maxwell DS, Tirado-Rives J. Development and testing of the OPLS all-atom force field on conformational energetics and properties of organic liquids. *J Am Chem Soc*. 1996;118:11225–11236.
12. Linse P. Monte Carlo simulation of liquid-liquid benzene-water interface. *J Chem Phys*. 1987;86:4177–4187.
13. Philpott MR, Glosli JN. Molecular dynamics simulation of the adsorption of benzene on charged metal electrodes in the presence of aqueous electrolyte. *Chem Phys*. 1995;198:53–61.
14. Schravendijk P, van der Vegt N, Delle Site L, Kremer K. Dual-scale modeling of benzene adsorption onto Ni (111) and Au(111) surfaces in explicit water. *Chem Phys Chem*. 2005;6:1866–1871.
15. Oostenbrink C, Villa A, Mark AE, van Gunsteren WF. A biomolecular force field based on the free enthalpy of hydration and solvation: the GROMOS force-field parameter sets 53A5 and 53A6. *J Comput Chem*. 2004;25:1656–1676.
16. Fischer J, Methfessel M. Born-Green-Yvon approach to the local densities of a fluid at interfaces. *Phys Rev A*. 1980;22:2836–2843.
17. MacKerell AD Jr, Brooks B, Brooks CB III, Nilsson L, Roux B, Won Y, Karplus M. CHARMM: the energy function and its parametrization with an overview of the program. In: Schleyer PvR, Allinger NL, Clark T, Gasteiger J, Kollman PA, Schaefer HF III, Schreiner PR, editors. *Encyclopedia of Computational Chemistry*, Vol. 1. Chichester: Wiley, 1998:271–277.
18. Lorentz HA. Ueber die Anwendung des Satzes vom Virial in der kinetischen Theorie der Gase. *Ann Physik*. 1881;2:127.
19. Berthelot D. Sur le Mélange des Gaz. *Compt Rend*. 1898;126:1703, 1857.
20. Martin MG. Comparison of the AMBER, CHARMM, COMPASS, GROMOS, OPLS, TraPPE and UFF force fields for prediction of vapour-liquid coexistence curves and liquid densities. *Fluid Phase Equilib*. 2006;248:50–55.
21. Steele WA. *The Interaction of Gases with Solid Surfaces*. Oxford: Pergamon Press, 1974.
22. Kolafa J. <http://www.vscht.cz/fch/software/macsimus>.
23. Berendsen HJC, Postma JPM, van Gunsteren WF, DiNola A, Haak JR. Molecular dynamics with coupling to an external bath. *J Chem Phys*. 1984;81:3684–3690.
24. Hsing HH, Wade WH. Weak interaction of cyclohexane with alumina. *J Colloid Interface Sci*. 1974;47:490.
25. Trzesniak D, Kunz APE, van Gunsteren WF. A comparison of methods to compute the potential of mean force. *Chem Phys Chem*. 2007;8:162–169.
26. Jarzynski C. Nonequilibrium equality for free energy differences. *Phys Rev Lett*. 1997;78:2690–2693.
27. Giles CH, Smith D, Huitson A. A general treatment and classification of the solute adsorption isotherm. I. Theoretical. *J Colloid Interface Sci*. 1974;47:755–765.
28. Radke CJ, Prausnitz JM. Thermodynamics of multi-solute adsorption from dilute liquid solutions. *AIChE J*. 1972;18:761–768.

Manuscript received July 9, 2007, revision received Feb. 22, 2008, and final revision received May 14, 2008.